Performance Degradation Effect Countermeasures in Residence Times Difference (RTD) Fluxgate Magnetic Sensors

Jingjie Li, *Member, IEEE*, Xue Zhang, *Member, IEEE,* Jiaqing Shi, Hadi Heidari, *Senior Member, IEEE*, and Yanzhang Wang

***Abstract*—This paper aims to explore the detection defect of residence times difference (RTD) fluxgate working in low-power mode. It presents the countermeasures for sensor resolution improvement and linearity enhancement. The main defects are amplitude and symmetry changes induced in the output spikes of fluxgate probe due to the magnetic field. These defects lead to thresholds deviation and asymmetry, then causes severe performance degradation especially on detection resolution and linearity according to the RTD theory. To overcome such effects, the optimized RTD method based on voltage extraction and feedback technology is proposed to implement magnetic field compensation and achieve a zero-field running regime of the RTD fluxgate. In this regard, the sensor linearity is improved by a factor of 38, and the resolution degradation effect is suppressed more than 6 times, verified by the laboratory experiments. The optimized detection method proposed in this paper demonstrated a great potential to achieve lower power consumption, will make the RTD fluxgate more promising technology among bio-magnetic applications.**

***Index Terms*—magnetic sensor, fluxgate sensor, residence times difference, symmetry broken, resolution improvement, linearity enhancement.**

I. Introduction

MAGNETIC sensors, have emerged as a promising new sensing technology in various biosensing applications for detection, identification, localization and manipulation of a wide spectrum of biological, physical and chemical agents in the past few years [1] – [4]. More stringent requirements for sensors have been put forward due to the unique working environment of biosensing, such as higher spatial resolution, more compact structure, and lower power consumption under the premise of fine sensitivity and detection resolution [3] - [6]. Fluxgates have been recognized as the most suitable vector magnetic field sensors for applications requiring a resolution up to 0.10 nT. However, the general spatial resolution of conventional fluxgate sensors is limited in several centimeters due to the complicated structure and say nothing of the vast excitation and bulky detection [7], [8]. State-of-the-art fluxgate sensors based on residence times difference (RTD), with the great potential to obtain the biosensing requirements, has been proposed and developed since 2003 [9] – [14]. The RTD fluxgate is based on the stochastic resonance phenomenon and quantifies the magnetic field by the measurement of the symmetry broken in the magnetic core. This operational scenario can provide a greatly simplified readout scheme, as well as significantly reduced processing procedures. And it can mitigate the effects of sensor noise and yield better performances in bistable noisy sensors compared with the harmonic detection [9]. The probe structure and detection system are both compact, and the fluxgate consumes less energy from the excitation. Furthermore, due to mechanical flexibility, the RTD fluxgate can be developed as a conformable sensor by using wire-core and can be an ideal potential use in wearable devices [15], [16].

During our recent experiments, we found that the sensor detection resolution and output linearity deteriorate with the magnetic field increasing. This degradation effect is especially severe when we try to reduce the amplitude of the excitation field to achieve lower power consumption.

In this paper, we investigate the detection defect of the RTD fluxgate working in low-power mode and present the countermeasures for sensor resolution improvement and linearity enhancement. The existence of the resolution and linearity degradation effect is identified through a customized setup and laboratory experiments. Through the modelling of the probe output and analysis of the detection method, the sources of the degradation effect are revealed. Furthermore, the effectiveness of the proposed countermeasures is proved by the experimental results, which demonstrate resolution

This manuscript was submitted at April 23, 2019. This work was supported in part by the National Key Research and Development Plan (Code No. 2018YFC1503903), and Graduate Innovation Fund of Jilin University. (*Corresponding author: Yanzhang Wang*)

Jingjie Li is with Key Laboratory of Geophysical Exploration Equipment (Jilin University), Ministry of Education of the People's Republic of China, and he is also with College of Instrumentation and Electrical Engineering, Jilin University, Changchun, China. (e-mail: jamin_lee@yeah.net).

Xue Zhang is with College of Instrumentation and Electrical Engineering, Jilin University, Changchun, China. (e-mail: zhangxue16@mails.jlu.edu.cn).

Jiaqing Shi is with College of Instrumentation and Electrical Engineering, Jilin University, Changchun, China. (e-mail: shijq17@mails.jlu.edu.cn).

Hadi Heidari is with School of Engineering, University of Glasgow, Glasgow G12 8QQ, UK. (e-mail: hadi.heidari@Glasgow.ac.uk).

Yanzhang Wang is with Key Laboratory of Geophysical Exploration Equipment (Jilin University), Ministry of Education of the People's Republic of China, and he is also with College of Instrumentation and Electrical Engineering, Jilin University, Changchun, China. (e-mail: yanzhang@jlu.edu.cn).

improvement and linearity enhancement for RTD fluxgate.

This paper is structured as follows. In Section II, the amplitude changes of induced output and asymmetry between positive- and negative spikes are analyzed theoretically. Section III describes the performance degradation effect and the optimization of the RTD method. In Section IV, the prototype of the optimized RTD fluxgate including probe and detection circuits is implemented. Finally, the experimental environment and results are presented in Section V.

II. METHODOLOGY

A. Modelling of Fluxgate Probe Output

The fluxgate probe is composed of the magnetic core, the solenoidal excitation coil and the induction coil. Considering the sinusoidal signal excitation,

$$H_e(t)=\frac{N_e}{l_e}i_e\sin\omega_e t=|H_e|\sin\omega_e t \tag{1}$$

where N_e and l_e are the turns and length of the excitation coil respectively, i_e and ω_e are the amplitude and frequency of the excitation current respectively, and $|H_e|=i_eN_e/l_e$ is the amplitude of the excitation magnetic field.

The magnetic field along the axis of the magnetic core can be described as the sum of excitation field $H_e(t)$ and target magnetic field $H_x(t)$, given by

$$H(t)=H_e(t)+H_x(t)=|H_e|\sin\omega_e t+H_x \tag{2}$$

where $H_x(t)$ is viewed as a static or quasi-static magnetic field.

The output of the probe can be easily modelled by Faraday's law, that is

$$e(t)=N_s\frac{d\varphi}{dt}=N_sS_s\frac{dB}{dt}=N_sS_s\frac{d[\mu(t)H(t)]}{dt} \tag{3}$$

where N_s is the turns of the induction coil, S_s is the effective area of the induction coil, φ is the magnetic flux, B is the magnetic flux density, and μ is the permeability of the magnetic core.

Combine (2) with (3), and by some mathematical derivation, we can get

$$e(t)=N_sS_s\left(\mu(t)\frac{dH_e}{dt}+(H_e+H_x)\frac{d^2B}{dH^2}\frac{dH_e}{dt}\right) \tag{4}$$

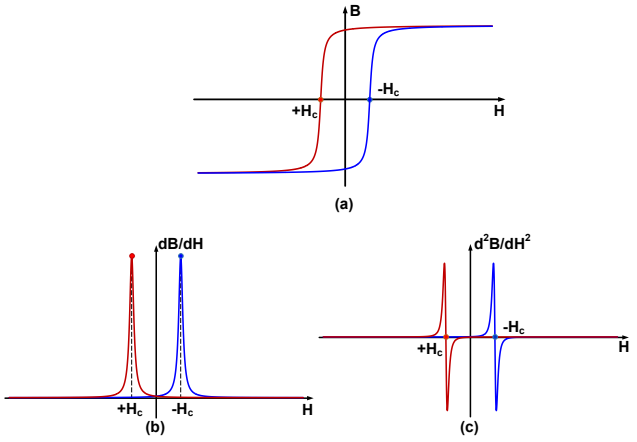

Fig. 1. (a) Hysteresis characteristic (B-H curve) of soft magnetic material, (b) the first order derivative of B to H, in other words, the magnetic permeability μ, (c) the second order derivative of B to H.

B. Magnetic Hysteresis of the Magnetic Core

The critical component of RTD fluxgate is the magnetic core and the hysteresis characteristic (B-H curve of magnetic material) shown in Fig. 1 (a) is the key theoretical support of fluxgate design.

Based on the shape features of the hysteresis loop shown in Fig.1, the arc tangent model is established via its trigonometric function [17] - [19], as shown in the following equation

$$B(H)=\alpha\bullet\arctan\left[\beta\bullet(H\pm H_c)\right] \tag{5}$$

where α is the saturation flux density parameter, and β is the permeability parameter.

The first and second order derivatives of B with respect to H can be derived from (5). That is,

$$\begin{cases}\dfrac{dB}{dH}=\dfrac{\alpha\bullet\beta}{\left[\beta\bullet(H\pm H_c)\right]^2+1}\\[2ex]\dfrac{d^2B}{dH^2}=\dfrac{-2\alpha\bullet\beta^3\bullet(H\pm H_c)}{\left[\beta^2\bullet(H\pm H_c)^2+1\right]^2}\end{cases} \tag{6}$$

where $dB/dH=\mu$ is the magnetic permeability.

Based on (6), the magnetic permeability and its rate of change are shown in Fig. 1 (b) and (c). As indicated in (6) and shown in Fig. 1, when the magnetic field $H(t)$ reaches to $\pm H_c$, the magnetic permeability $\mu=dB/dH$ will arrive at its maximum value μ_{max}, and the second order derivative will reach to zero. That is,

$$\begin{cases}\left|\mu=\dfrac{dB}{dH}\right|_{H=|H_c|}=\mu_{max}\\[2ex]\dfrac{d^2B}{dH^2}\Big|_{H=|H_c|}=0\end{cases} \tag{7}$$

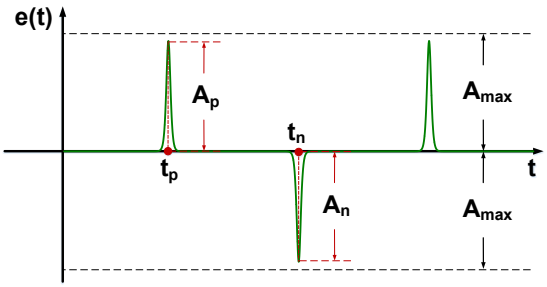

Fig. 2. The induced output and spikes of RTD fluxgate probe.

C. Amplitude Change of the Induced Output

Indicated in (4) and (7), when $H(t)=|H_c|$, the magnetic flux density ($B=\mu H$) will experience rapid jumps, which appear as spikes in the induced signal of the induction coil as shown in Fig. 2. And the time differences between the positive spikes and negative spikes are the key information carriers for RTD fluxgate [10] – [13].

Combine (7) with (4),

$$e_{(H=|H_c|)}=N_sS_s\mu_{max}|H_e|\omega_e\cos\omega_e t \tag{8}$$

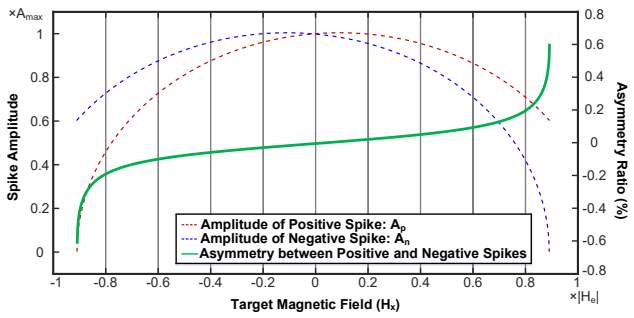

Fig. 3. The amplitude changes of the induced signal (dashed lines), and the amplitude asymmetry between positive- and negative spikes (solid line).

The times when spikes occur are evaluated by,

$$\begin{cases} |H_e|\sin\omega_e t_p + H_x = H_c \\ |H_e|\sin\omega_e t_n + H_x = -H_c \end{cases} \tag{9}$$

Then we get

$$\begin{cases} t_p = \dfrac{1}{\omega_e}\arcsin\dfrac{H_c - H_x}{|H_e|} \\ t_n = \dfrac{1}{\omega_e}\arcsin\dfrac{-H_c - H_x}{|H_e|} \end{cases} \tag{10}$$

where $-|H_e|+H_c<H_x<|H_e|-H_c$.

Combine (10) with (8), the amplitude of spikes can be determined,

$$\begin{cases} A_p = e_{(H=H_c)} = |e(t_p)| = N_s S_s \mu_{\max} |H_e| \cos\left(\arcsin\dfrac{H_c - H_x}{|H_e|}\right) \\ A_n = e_{(H=-H_c)} = |e(t_n)| = N_s S_s \mu_{\max} |H_e| \cos\left(\arcsin\dfrac{H_c + H_x}{|H_e|}\right) \end{cases} \tag{11}$$

From (11), when $H_x=H_c$, the amplitude of the positive spike gets its maximum value $A_{p\_\max}$, and when $H_x=-H_c$, the amplitude of the negative spike gets its maximum value $A_{n\_\max}$. And $A_{p\_\max} = A_{n\_\max} = A_{\max}$ from (11).

$$A_{p\_\max} = A_{n\_\max} = e_{(H_x=H_c)} = N_s S_s \mu_{\max} |H_e| \tag{12}$$

According to (12), the amplitude changes of the induced signal calculated by MATLAB is shown in Fig. 3. The amplitude changes of positive- and negative spikes are obvious, especially when the target magnetic field $|H_x|$ is large.

The asymmetry can be given as the amplitude difference between positive- and negative spikes.

$$R_{asy} = \frac{A_p - A_n}{A_{\max}} = \cos\left(\arcsin\frac{H_c - H_x}{|H_e|}\right) - \cos\left(\arcsin\frac{H_c + H_x}{|H_e|}\right) \tag{13}$$

where R_{asy} is the asymmetry ratio of the induced output.

The asymmetry of the induced signal can be numerically calculated by MATLAB in light of (13) shown as solid line in Fig. 3. The amplitude asymmetry of positive- and negative spikes is obvious gradually along with $|H_x|$ increasing, especially the target magnetic field H_x is large. And only when $H_x=0$, the positive spike is symmetric with the negative spike.

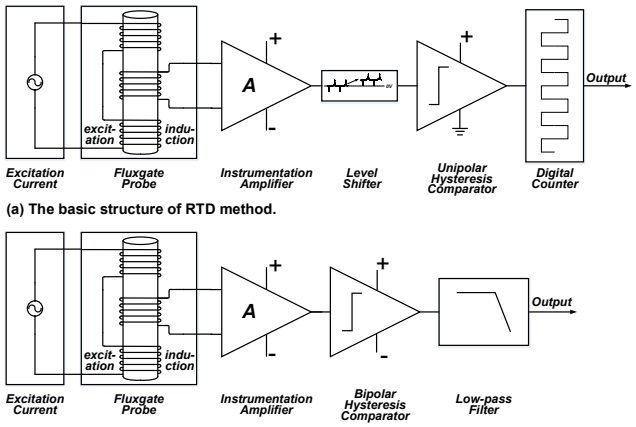

Fig. 4. The basic structure of RTD method and the voltage extraction of the optimized RTD method.

III. Performance Degradation and Optimization

A. The Magneto-Sensitive Resolution of RTD Method

The RTD fluxgate is basically consisted of the excitation current, the fluxgate probe, the amplifier, the hysteresis comparator, and the digital counter, as shown in Fig. 4 (a). According to the RTD detection theory [12], [13], [25], [26], the positive threshold V_{tp} and negative threshold V_{tn} of the hysteresis comparator should be symmetric and fixed, $V_{tp}=-V_{tn}=V_t$. Because the noise of the RTD probe output is not uniformly distributed [20] – [23], so the detection resolution is threshold sensitive.

The resolution of RTD fluxgate can be determined by the mean-square method, given by

$$R_{\text{mag}} = \frac{\text{std}(\overline{\text{RTD}_t^q})}{S} \tag{14}$$

where std is the standard deviation operator, t represents the observation/average time, q counts the events on which the standard deviation is estimated, and S is the sensor sensitivity [16], [24].

Here, the hysteresis threshold is defined as the ratio of the threshold voltage of comparator to the amplitude of the spike signal. Based on (14), the relationship between the detection resolution and the hysteresis threshold is determined by the

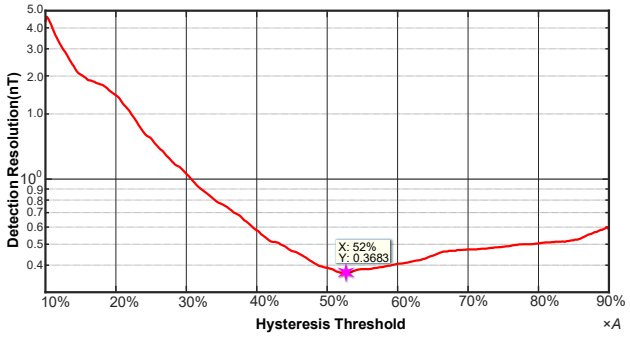

Fig. 5. The measured relationship between hysteresis threshold and detection resolution. A is the amplitude of the output spikes. The observation time is set to be 1s.

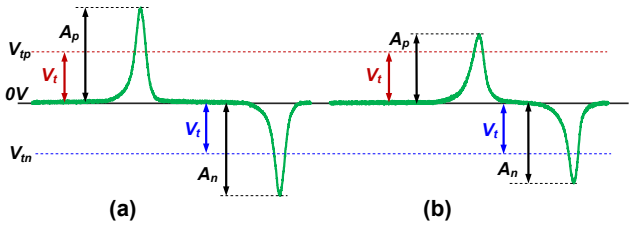

Fig. 6. Illustration of the Detection defects. (a) The detection condition when H_x=0; (b) the condition when H_x≠0. The two signals are both in one period.

numerical method, and the result is shown in Fig. 5. There is a turning point in the relationship curve between the detection resolution and hysteresis threshold. We can obtain that the detection resolution improves rapidly with the increase of the hysteresis threshold until reaching the turning point. And after that, the detection resolution starts getting a slight deterioration. According to our experiment data, the threshold turning point is 52%A, and the corresponding detection resolution is about 0.36nT. Therefore, we draw a conclusion that the hysteresis threshold has to be consistent with the turning point in order to attain the best detection resolution, in which circumstance, we define it as the optimal threshold value.

According to the RTD detection method general principle, the positive threshold V_{tp} and negative threshold V_{tn} of the hysteresis comparator are symmetrical with respect to the reference voltage, as shown in Fig. 6. We give the symmetrical and fixed thresholds considering the effects caused by the target magnetic field. Combine the information presented in Fig. 6 with results of Section II, the amplitude and asymmetry of the output spikes are influenced by the target magnetic field, and their variation influences the hysteresis thresholds. Then, the thresholds will deviate from the optimal value because of the amplitude changes. And the symmetry between the positive- and negative thresholds, which is the necessary condition for feasibility the RTD theory, will be broken because the asymmetry of the induced signal is generated. Finally, the detection resolution and accuracy will deteriorate due to the detection defect of the traditional RTD method.

B. The Optimized RTD Method based on Voltage Extraction and Feedback Technology

From the discussion aforementioned, the RTD fluxgate can obtain the best performances when the device is working at zero-magnetic-field state. However, with the target magnetic field varying, the amplitude of spikes changes, generating asymmetry effect and causing performance degradation. Given the fact that the main reason of the afore confirmed defects is the existence of the non-zero magnetic field around the magnetic core, utilizing feedback technique as a magnetic field compensation to realize zero-field around the magnetic core is crucial to maintain the best performances at full sensor scale.

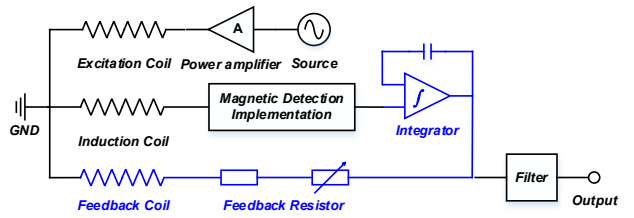

Fig. 7. The structure of fluxgate magnetometer with feedback technology utilized. The blue part including an integrator, feedback resistor and feedback coil is the feedback branch.

As shown in Fig. 7, the designed feedback branch consists of an integrator, a feedback resistor, and a feedback coil. With the feedback branch added, the fluxgate forms a closed loop system. The applied magnetic field is generated by a feedback branch to actively zero the field around the magnetic core and the exploitation of an integrator makes it possible to detect the target magnetic field at the same time.

For the RTD method shown in Fig. 4 (a), the digital output, as a major advantage of the RTD method, makes it difficult to compatible with the feedback fluxgate unless using digital-to-analog (DA) converter. In order to realize the voltage output and maintain the simplicity of RTD method, we optimized the RTD method by removing the digital counter and adding a low-pass filter to extract the DC component and suppress the interference brought by the excitation signal, as shown in Fig. 4 (b).

From the discussion in II and illustration in Fig. 2, the saturation times can be sorted as,

$$\begin{cases} t_p = \dfrac{1}{\omega_e}\arcsin\dfrac{H_c - H_x}{|H_e|} \\ t_n = \dfrac{1}{\omega_e}\arcsin\dfrac{H_c + H_x}{|H_e|} + \dfrac{\pi}{\omega_e} \\ t_{pn} = \dfrac{1}{\omega_e}\arcsin\dfrac{H_c + H_x}{|H_e|} + \dfrac{2\pi}{\omega_e} \end{cases} \tag{15}$$

where t_{pn} is the positive saturation time of the next period.

The saturation accumulation S_A in one period can be calculated as,

$$\begin{aligned} S_A &= \int_{t_p}^{t_{pn}} B dt = B_s\left(t_n - t_p\right) - B_s\left(t_{pn} - t_n\right) \\ &= \frac{2B_s}{\omega_e}\left(\arcsin\frac{H_c + H_x}{|H_e|} - \arcsin\frac{H_c - H_x}{|H_e|}\right) \end{aligned} \tag{16}$$

With the field compensation achieved, the magnetic field in the area of magnetic core will be near-zero when the feedback system reaches its stable equilibrium. Then, the output of the optimized RTD method can be calculated as Taylor's expression at H_x=0, given as

$$S_A \approx \frac{4B_s}{\omega_e\sqrt{|H_e|^2 - H_c^2}} H_x \tag{17}$$

As shown in Fig. 7, as long as the forward gain of the feedback system is large enough, the output of the fluxgate magnetometer will be only relevant to the parameters of the feedback branch when the feedback system is stable,

$$V_{out} = \frac{L_F\left(R_{FC} + R_F\right)}{\mu_0 N_F} H_x \tag{18}$$

By the optimization of RTD method based on voltage extraction and feedback technology described above, the fluxgate can work as a closed-loop system. The magnetic field

around magnetic core keeps zero all the time regardless the actual value of external field owing to the active countervailing capacity guaranteed by feedback, which means that the output spikes of fluxgate probe will be symmetrical and the amplitudes will remain unchanged. Therefore, the threshold of hysteresis comparator can be accurately set at its optimal value, and the magnetometer can obtain the best detection resolution at full scale.

IV. Fabrication and Implementation

A. Design of the Fluxgate Probe

The fluxgate probe consists of the support skeleton, magnetic core, excitation coil, induction coil and feedback coil as shown in Fig. 8. The support skeleton is made of the nonmagnetic resin, and all the coils are designed as solenoid type coils. The detailed parameters of the probe are given in Table I.

B. Circuits Design for the Optimized RTD Method

The detection circuits are designed according to the structure of the optimized RTD method shown in Fig. 4 (b) and Fig. 7. The detection circuits are shown in Fig. 9. The detection circuit is composed of six parts. Firstly, the signal from the RTD fluxgate probe is coupled by high-pass coupling circuit (Fig. 9 (a)) which can remove the DC offset and provide the necessary current return path for the instrumentation amplifier (Fig. 9 (b)). After the pre-amplification, the analog hysteresis comparator (Fig. 9 (c)) is utilized to realize RTD detection. Then, the DC extraction (Fig. 9 (d)) is implemented by a 5th-order low-pass filter with a cut-off frequency of 10Hz. The amplifier (Fig. 9 (e)) provides the sufficient gain to reduce the system response time. Finally, after a leaky integrator (Fig. 9 (f)), the signal is fed back to the feedback coil to offset the target magnetic field. When the detection system reaches its equilibrium state, the target magnetic field will be totally counteracted and the fluxgate will work in the zero-field state, and the output of the integrator will be in proportion to the target magnetic field indicated by (18).

The analog hysteresis comparator design is the most important part of our threshold sensitivity detection. By some circuit analysis, the hysteresis threshold of the analog comparator shown in Fig. 9 (c) can be written as

$$\begin{cases} V_{T+} = \dfrac{R4\left(V_{F1}+V_{Z2}\right)}{R4+R5} \\ V_{T-} = \dfrac{-R4\left(V_{Z1}+V_{F2}\right)}{R4+R5} \end{cases} \tag{19}$$

Where V_{T+} is the positive threshold, V_{T-} is the negative threshold, V_{F1} is the forward voltage of diode D_1, V_{Z1} is the regulation voltage of D_1, V_{F2} is the forward voltage of diode D_2, V_{Z2} is the regulation voltage of D_2.

Firstly, the output signal of the sensor probe is amplified by the pre-amplifier (Fig. 9 (c)) to be V_{sig_max}=+4 V and V_{sig_min}=-4 V. And as shown in Fig. 9 (c), with R4=51 KΩ, R5=47 KΩ, D1 and D2 using the precision Zener diode IN5226 produced by Motorola, the thresholds can be uniquely determined by (19).

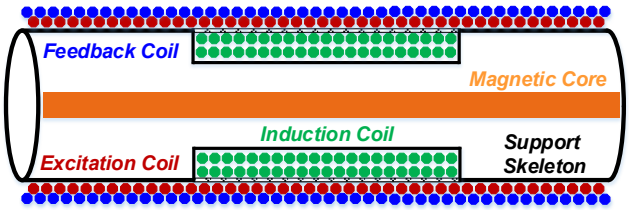

Fig. 8. The structure of the fluxgate probe. The white part with the black line, yellow part, red part, green part, and blue part represents the support skeleton, magnetic core, excitation coil, induction coil, and feedback coil respectively.

TABLE I
Detailed Parameters of the Fluxgate Probe

Magnetic Core	**Characteristics**	
	Value	*Units*
Material	cobalt-based amorphous alloy ribbon	
Width	0.8	mm
Thickness	20	μm
Length	60	mm
Saturation Induction	0.57	T
Maximum Permeability	≥1000000	Gs/Oc
Coercive Force	<2.2	A/m
Excitation Coil	**Characteristics**	
	Value	*Units*
Material	0.1mm enameled copper wire	
Turns	200	
Coil Internal Radius	1.8	mm
Induction Coil	**Characteristics**	
	Value	*Units*
Material	0.1mm enameled copper wire	
Turns	1000	
Coil Internal Radius	2.0	mm
Feedback Coil	**Characteristics**	
	Value	*Units*
Material	0.1mm enameled copper wire	
Turns	600	
Coil Internal Radius	2.2	mm
Support Skeleton	**Characteristics**	
	Value	*Units*
Material	resin	
Width	8	mm
Height	8	mm
Length	80	mm

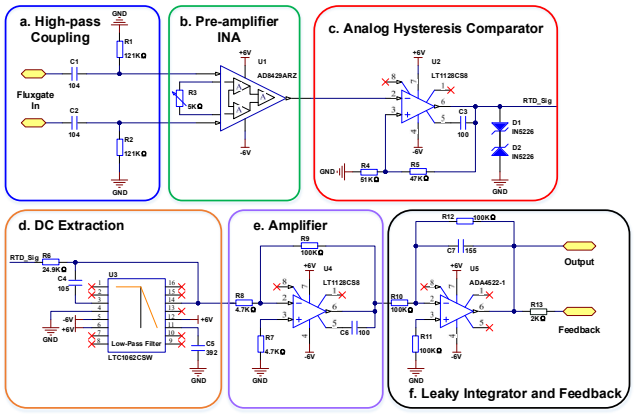

Fig. 9. The detection circuit of optimized RTD method.

$$\begin{cases} V_{T+} = \dfrac{51K\Omega(0.7V+3.3V)}{51K\Omega+47K\Omega} \approx 2.08V = 52\%V_{sig\_\max} \\ V_{T-} = \dfrac{-51K\Omega(3.3V+0.7V)}{51K\Omega+47K\Omega} \approx -2.08V = 52\%V_{sig\_\min} \end{cases} \quad (20)$$

Corresponding to the optimal hysteresis thresholds analyzed in Sec. III, the analog hysteresis comparator designed in this part can realize the optimal threshold (52%) and obtain the best detection resolution.

V. Experimental Results

A. Experimental Environment

In order to provide a proper experimental environment for the evaluation of sensor performances, the electromagnetic (EM) shielded room which has 40 dB attenuation for the static magnetic field (e.g. the geomagnetic field) and 60 dB attenuation for 50 Hz power line interference and an EM shielded barrel which has 60 dB attenuation for the static magnetic field are employed. In the experiments, the EM shielded barrel is placed in the EM shielded room, and the sensor probe is placed in the centre of the EM shielded barrel. After demagnetization, the residual of the static magnetic field is less than 1 nT and the fluctuation is less than 0.01 nT inside the EM shielded barrel. And the detailed experimental setup is shown in Fig. 10. A Helmholtz coil to generate the magnetic field for the sensor calibration, a Keithley 6221 current source to provide the bias current for sensor probe, a power device for power supply, and a data acquisition system (DAQ) USB4431 produced by National Instruments with a computer for signal recording are employed. The bias signal given by Keithley 6221 for sensor probe is the sinusoidal wave with amplitude 15 mA and frequency 600 Hz. Additionally, the dimension of the detection circuit is about 3cm×5cm much smaller compared with the RTD detection circuits with FPGA counter.

B. Sensor Calibration and Linearity Evaluation

The sensor calibration has been carried out by setting different target magnetic fields and recording the sensor outputs in the given experimental environment described above. Both the fluxgate with optimized RTD method (F_1) proposed in this article and with the traditional RTD method (F_0) are tested,

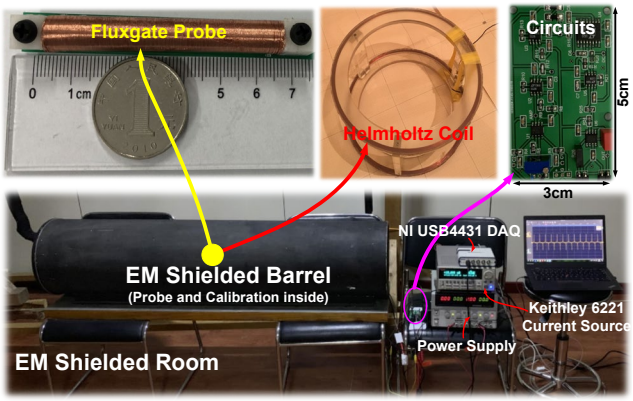

Fig. 10. The experimental setup, including the experimental environment, experimental instrumentation, fluxgate probe, and detection circuits.

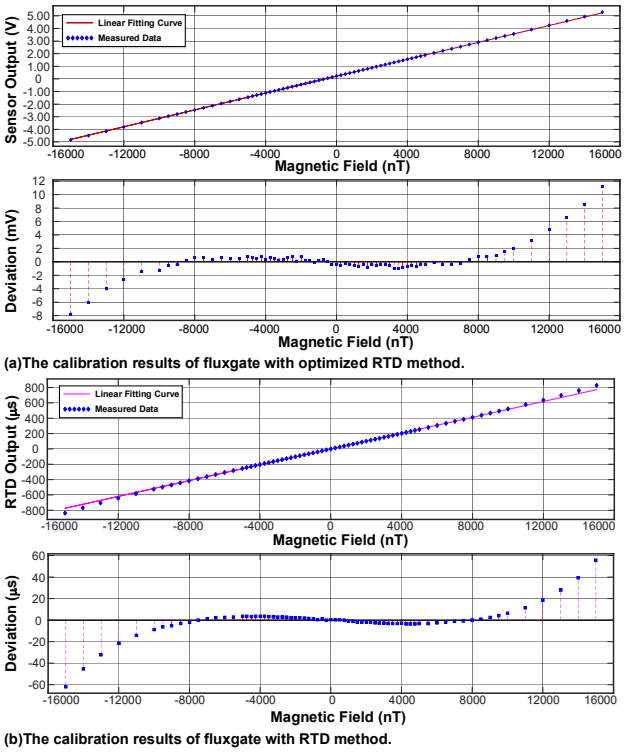

Fig. 11. The calibration results. The upper two are the results of fluxgate with optimized RTD method, and the bottom two are the results of fluxgate with RTD method.

TABLE II
Linear Fitting Results: Sensor Sensitivity & Deviation

Items	Fluxgate with Optimized RTD Method (F_1)	Fluxgate with Traditional RTD Method (F_0)
Sensitivity(S)	334.5 μV/nT	51.6 ns/nT
Maximum Deviation ($\triangle L_{\max}$)	11.2 mV	62 μs
Full Scale Output ($Y_{F.S}$)	5.29 V	774.48 μs

and the results are shown in Fig. 11. Fig. 11 (a) is the calibration results of F_1 and Fig. 11 (b) is the calibration results of F_0. In addition, the output of fluxgate F_1 is voltage-type, while that of fluxgate F_0 is time-type. Here, the hysteresis threshold is set to be 52%A initially. The thresholds of F_1 will be kept consistent with the increase of the magnetic field, while that of F_0 will be changed and asymmetrical due to the aforementioned probe output changing and asymmetry generating in Section II.

Linear fitting of the results using the least squares method can obtain the sensor sensitivity and output deviation. The sensitivity and output deviation are listed in Table II. In Fig. 11, the degradation effect on sensor linearity and output deviation is clearly presented which is consistent with the prediction of Sec. III.

The nonlinearity of sensor (ξ_L) is defined by the ratio of maximum deviation ($\triangle L_{\max}$) to full-scale output ($Y_{F.S}$), given by

$$\xi_L = \pm \frac{\Delta L_{\max}}{Y_{F.S}} \times 100\% \quad (21)$$

Calculated by (21), the nonlinearity of fluxgate F_1 is 0.21%, while that of fluxgate F_0 is 8.01%. The bad linearity of fluxgate F0 is mainly due to the symmetry broken between the positive and negative thresholds predicted in Sec. III. The asymmetry

thresholds make the RTD theory infeasible for field estimation, therefore causing severe deviation to the exact value of the magnetic field. And with the optimize RTD method utilized, the symmetry of the probe output spikes will be highly maintained, and then the thresholds symmetry will be greatly enhanced, therefore the deviation will be decreased and the fluxgate will obtain better linearity.

C. Resolution Enhancement

Based on (14), the sensor magnetic resolution can be estimated, and the results are shown in Fig. 12. The resolution of the fluxgate with RTD method is severely affected by the magnetic field, which varies from 0.39 nT to 1.57 nT when the magnetic field changes from 0 to ±15000 nT. With the optimized RTD method utilized, the degradation of magnetic resolution is mitigated, and the resolution responsively varies from 0.30 nT to 0.48 nT among the full scale. In addition, the resolution at zero magnetic fields is improved, from 0.39 nT to 0.30 nT, mainly benefits from the low-pass filter utilization in the optimized RTD detection circuits. Here, the resolution degradation factor F_{rd} which shown the severity of the resolution degradation effect is defined and given by

$$F_{RD} = \frac{\Delta R_{\max}}{R_0} = \frac{(R - R_0)_{\max}}{R_0} \times 100\% \tag{22}$$

where R is the resolution data among the full sensor scale, and R_0 is the resolution at zero magnetic fields.

The resolution improvement factor F_{RI} to demonstrate the effectiveness of the optimized method is calculated by

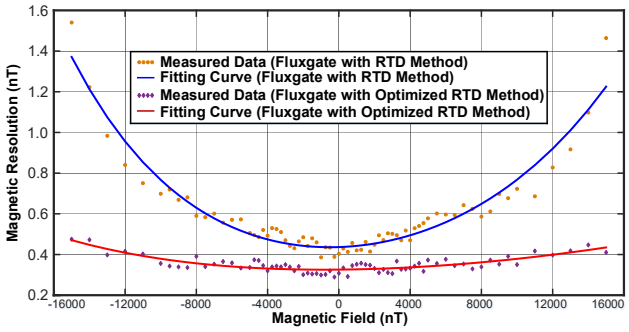

Fig. 12. Experiments obtained magnetic resolution. The yellow and purple dots represent the measured data of fluxgate F_0 and fluxgate F_1 respectively. And the blue and red lines represent the curve fitting of F_0 and F_1 respectively. The observation time is set to be 1s.

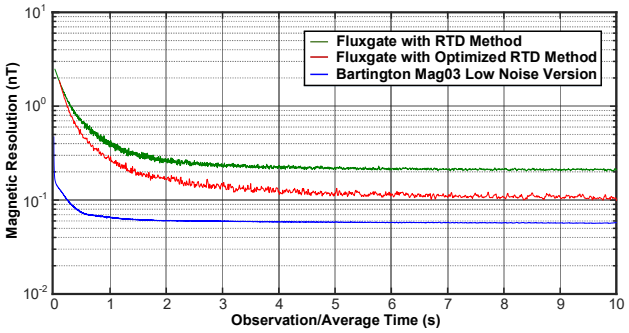

Fig. 13. Magnetic resolution of the sensor versus the observation time.

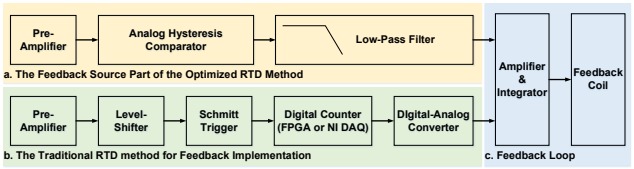

Fig. 14. Two methods to implement the feedback technology for RTD fluxgate.

$$F_{RI} = \frac{F_{RD}^{tra}}{F_{RD}^{opt}} = \frac{R_0^{opt}\left(R^{tra} - R_0^{tra}\right)_{\max}}{R_0^{tra}\left(R^{opt} - R_0^{opt}\right)_{\max}} \times 100\% \tag{23}$$

where F_{RD}^{tra} and F_{RD}^{opt} are the resolution degradation factor of the traditional and optimized RTD method respectively.

Combine (23) with the data from Fig. 12, $F_{RI} \approx 6.55$ indicates that the resolution degradation effect is suppressed more than 6 times after the optimized RTD method utilized.

Taking the observation time into account, an estimation of the magnetic resolution as a function of the observation time is obtained, and the results are shown in Fig. 13. The fluxgate with optimized RTD method has better magnetic resolution compared with the fluxgate with traditional RTD method. By considering an observation window of 5 s, a resolution around 0.10 nT can be obtained for the fluxgate with optimized RTD method. Although the fluxgate with optimized RTD method is still not comparable to the sophisticated Mag03 fluxgate, it can find applicability on low-cost applications.

VI. Discussion

As for RTD fluxgate, the magnetic resolution and linearity degradation resulting from amplitude change of the induced output and asymmetry between positive and negative spikes is mainly due to the deviation of thresholds from its optimal value and the symmetry broken between the positive and negative thresholds caused by the existence of magnetic field around the magnetic core. Developing a magnetic field compensation method based on feedback technology so that the magnetic core works in the zero-magnetic environment is feasible to ease this degradation effect.

To implement the feedback system, the first challenge is to find a suitable feedback source which generally is the voltage signal. **As shown in Fig. 14**, there are two simple methods to implement this compensation function. One is implementing the RTD detection using the digital method and then using the DA converting technology to generate the voltage output. This method makes the detection system complex and bulky which violates the original design intention of the RTD fluxgate [12], [13], [27]. The other one is using the optimized RTD method proposed in this article to form the direct voltage output. The fluxgate with the optimized RTD method has been designed, fabricated and tested in our well-designed magnetic shielding environment. The optimization exhibits linearity enhancement and resolution improvement for RTD fluxgate which has been verified by laboratory experiments. Furthermore, with this optimized method utilized, the RTD fluxgate can achieve lower power consumption by reducing the amplitude of excitation.

The fluxgate utilizing the optimized RTD method has

advantages of small size and simple probe structure and can obtain better performances compared with the traditional RTD fluxgate. The voltage-type output is more compatible in sensor design, and it has great advantages in the hybrid design of different sensors to obtain expanded performances, such like the hybrid design of fluxgate and induction coils sensor to extend the frequency bandwidth with lower detection noise [28] – [30].

VII. Conclusion

This paper presented an optimization method based on voltage extraction and feedback technology for the RTD fluxgate. Firstly, the amplitude changes and asymmetry effect of the probe output caused by the magnetic field was investigated. Then, according to the traditional RTD method, the resolution degradation effect was determined. And to ease this effect and realize the optimal magnetic resolution among the full sensor scale, the optimization of the RTD strategy was proposed. **Afterward, the fluxgate with optimized RTD method was designed**, realized, and characterized. Finally, the sensor linearity is improved by a factor of 38, and the detection resolution is improved from 0.39 nT to 0.30 nT and from 1.57 to 0.48 nT for zero magnetic field and huge magnetic field respectively. The resolution degradation effect is suppressed more than 6 times. Therefore, the validation of the optimized method for RTD fluxgate is verified.

For the first time, a closed-loop system in the RTD fluxgate is implemented. The experimental results verify the existence of detection degradation effect, indicate the enhancements in sensor linearity and magnetic resolution, and reveal the feasibility of an optimized method in the RTD fluxgate design. And the optimization proposed brings about the great potential to achieve lower power consumption, which will make the RTD fluxgate obtain more promising attractions among bio-magnetic applications.

References

[1] V. Nabaei, R. Chandrawati, and H. Heidari, "Magnetic biosensors: Modelling and simulation," *Biosens. Bioelectron.*, vol. *103*, pp. *69-86*, Apr. 2018.

[2] J. Ali, J. Najeeb, M. A. Ali, and et al., "Biosensors: their fundamentals, designs, types and most recent impactful applications: a review," *J. Biosens. Bioelectron.*, vol. *8*, no. *1*, pp. *1-9*, Jan. 2017.

[3] H. Heidari, "Electronic skins with a global attraction," *Nat. Electron.*, vol. *1*, pp. *578-579*, Nov. 2018.

[4] J. C. Rife, M. M. Miller, P. E. Sheehan, and et al., "Design and performance of GMR sensors for the detection of magnetic microbeads in biosensors," *Sens. Actuators, A*, vol. *107*, no. *3*, pp. *209-218*, Nov. 2003.

[5] A. V. Reenen, A. M. D. Jong, J. M. J. D. Toonder, and et al., "Integrated lab-on-chip biosensing systems based on magnetic particle actuation–a comprehensive review," *Lab Chip*, vol. *14*, pp. *1966-1986*, Mar. 2014.

[6] A. Sandhu, "Biosensing: new probes offer much faster results," *Nat. Nanotechnol.*, vol. *2*, pp. *746-746*, Dec. 2007.

[7] J. Lenz, and A. S. Edelstein, "Magnetic sensors and their applications," *IEEE Sens. J.*, vol. *6*, no. *3*, pp. *631-649*, Jun. 2006.

[8] P. Ripka, "New directions in fluxgate sensors," *J. Magn. Magn. Mater.*, vol. *215*, pp. *735-739*, Jun. 2000.

[9] A. Nikitin, N. G. Stocks, A. R. Bulsara, "Bistable sensors based on broken symmetry phenomena: The residence time difference vs. the second harmonic method," *The European Physical Journal Special Topics*, vol. *222*, no. *10*, pp. *2583-2593*, Oct. 2013.

[10] A. R. Bulsara, C. Seberino, L. Gammaitoni, and et al., "Signal detection via residence-time asymmetry in noisy bistable devices," *Phys. Rev. E*, vol. *67*, no. *1*, pp. *1-21*, Jan. 2003.

[11] A. Nikitin, N. G. Stocks, and A. R. Bulsara, "Signal detection via residence times statistics: Noise-mediated minimization of the measurement error," *Phys. Rev. E*, vol. *68*, no. *3*, pp. *1-4*, Sept. 2003.

[12] B. Andò, S. Baglio, A. R. Bulsara, and et al., ""Residence times difference" fluxgate magnetometers," *IEEE Sens. J.,* vol. *5*, no. *5*, pp. *895-904*, Oct. 2005.

[13] B. Andò, S. Baglio, V. Caruso, and et al., "Multilayer based technology to build RTD fluxgate magnetometer," *Sens. Transducers J.*, vol. *65*, no, *3*, pp. *509-514*, Mar. 2006.

[14] B. Andò, A. Ascia, S. Baglio, and et al., "Towards an optimal readout of a residence times difference (RTD) fluxgate magnetometer," *Sens. Actuators, A*, vol. *142*, no. *1*, pp. *73-79*, Mar. 2008.

[15] B. Andò, S. Baglio, A. R. Bulsara, and et al., "Design and characterization of a microwire fluxgate magnetometer," *Sens. Actuators, A*, vol. *151*, no. *2*, pp. *145-153*, Apr. 2009.

[16] C. Trigona, V. Sinatra, B. Andò, and et al., "Flexible microwire residence times difference fluxgate magnetometer," *IEEE Trans. Instrum. Meas.*, vol. *66*, no. *3*, pp. *559-568*, Mar. 2017.

[17] H. Trujillo, J. Cruz, M. Rivero, and et al., "Analysis of the fluxgate response through a simple spice model," *Sens. Actuators, A*, vol. *75*, no. *1*, pp. *1-7*, May. 1999.

[18] Y. Wang, S. Wu, Z. Zhou, and et al., "Research on the dynamic hysteresis loop model of the residence times difference (RTD)-fluxgate," *Sens.*, vol. *13*, no. *9*, pp. *11539-11552*, Aug. 2013.

[19] F. C. F. Guerra, and W. S. Mota, "Magnetic core model," *IET Sci. Meas. Technol.*, vol. *1*, no. *3*, pp. *145-151*, 2007.

[20] E. Weiss, R. Alimi, A. Ivry, and et al., "Investigation and Modelling of Large Barkhausen Jumps Dynamics in Low-Power Fluxgate Magnetometers," *IEEE Sens. J.*, vol. *19*, no. *6*, pp. *2105-2112*, Mar. 2018.

[21] J. L. M. J. V. Bree, J. A. Poulis, and et al., "Barkhausen noise in fluxgate magnetometers," *Appl. Sci. Res.*, vol. *29*, no. *1*, pp. *59-68*, Jan. 1974.

[22] M. Butta, S. Yamashita, and I. Sasada, "Reduction of noise in fundamental mode orthogonal fluxgates by optimization of excitation current," *IEEE Trans. Magn.*, vol. *47*, no. *10*, pp. *3748-3751*, Oct. 2011.

[23] G. P. Farrell, and E. W. Hill, "The limit of fluxgate sensitivity due to Barkhausen noise for single layer and bi-layer permalloy thin film cores," *IEEE Trans. Magn.*, vol. *31*, no. *6*, pp. *4050-4052*, Nov. 1995.

[24] J. Li, Y. Wang, X. Zhang, and et al., "Sensitivity and Resolution Enhancement of Coupled-Core Fluxgate Magnetometer by Negative Feedback," *IEEE Trans. Instrum. Meas.*, vol. *68*, no. *2*, pp. *623-631*, Feb. 2019.

[25] B. Andò, S. Baglio, V. Sacco, and et al., "Noise effects in RTD-fluxgate," in *Sensors., IEEE*, Irvine, USA, *2005*, pp. *935-938*.

[26] S. Baglio, V. Sacco, and A. R. Bulsara, "Read-out circuit in RT-fluxgate," in *Int. Circuits and Systems., IEEE*, Kobe, Japan, 2005, pp. 5910-5913.

[27] B. Andò, S. Baglio, A. R. Bulsara, and V. Sacco, "RTD fluxgate: A low-power nonlinear device to sense weak magnetic fields," *IEEE Instrumentation & Measurement Magazine*, vol. *8*, no. *4*, pp. *64-73*, Oct. 2005.

[28] F. Han, S. Harada, and I. Sasada, "Fluxgate and search coil hybrid: A low-noise wide-band magnetometer," *IEEE Trans. Magn.*, vol. *48*, no. *11*, pp. *3700-3703*, Nov. 2012.

[29] P. Brown, B. J. Whiteside, T. J. Beek, and et al., "Space magnetometer based on an anisotropic magnetoresistive hybrid sensor," *Rev. Sci. Instrum.*, vol. *85*, no. *12*, pp. *1-9*, Dec. 2014.

[30] C. Coillot, J. Moutoussamy, G. Chanteur, and et al., "On-board hybrid magnetometer of NASA CHARM-II rocket: principle, design and performances," *J. Sens. Sens. Syst.*, vol. 2, no. 2, pp. 137-145, Jun. 2013.